COBEM 2021 26th International Congress of Mechanical Engineering
November 22-26, 2021, Virtual Congress, Brazil

COB-2021-0990
A COMPARATIVE ANALYSIS BETWEEN AMMONIA-WATER ABSORPTION AND VAPOR COMPRESSION REFRIGERATION SYSTEMS

Wellorzzon Ronnan Ibide Novais
Erick Pereira Cerqueira
Beethoven Narváez-Romo
José Roberto Simões-Moreira
SISEA - Renewable and Alternative Energy Systems Laboratory
Mechanical Engineering Department – Escola Politécnica of the University of São Paulo
Av. Professor Mello Moraes, 2231, CEP 05508-030 – São Paulo – SP – Brazil
wellorzzon.novais@usp.br, erickcerqueira@usp.br, betonarmo@gmail.com, jrsimoes@usp.br

Abstract. *Refrigeration systems applications are broadly used in food and drug conservation and air conditioning. Commercial buildings demand up to 80% of total electrical power just for powering air-conditioning based on conventional vapor compression refrigeration systems (VCRS), which contributes to reach peaks on the electrical distribution network that could cause an unstable condition. Implementing absorption refrigeration systems (ARS) producing cooling effect driven by thermal energy could decrease this power consumption. Thermodynamic models of these systems can be found in the literature with a variety of working fluids and also integrated with other cycles such as power generation plants, however, just some have a direct comparison between ARS and VCRS employing the same conditions. Thus, the current study aims to simulate and compare two different types of refrigeration technologies: single stage ammonia-water absorption refrigeration cycle, and vapor compression refrigeration cycle working with R-134a and R-717. Thermodynamic simulation was carried out by evaluating heat transfer rates of main devices, coefficients of performance and specific areas of evaporator and condenser. As evaporator temperature decreases, ARS requires 16.9 kW or 67.5% more heat in generator and COP decreased from 0.601 to 0.359. Utilizing the same comparison parameter, VCRS needed 3.26-3.54 kW or 154-160% more compressor power, depending on refrigerant used, and COP decreased from 6.77 to 2.60 with R-134a and 7.07 to 2.79 using R-717. Compared to ARS, condenser specific area required for VCRS is smaller, evaporator is two times smaller when using R-134a, and is equal when using R-717. Those results can justify the usage of ARS in facilities with high amount of heat waste, mainly on applications working with lower evaporator temperatures.*

Keywords: *absorption refrigeration cycle, compression refrigeration cycle, thermodynamic simulation, heat transfer, ammonia-water*

1. INTRODUCTION

Refrigeration systems are used in various applications, such as food or drug conservation and air-conditioning to increase thermal comfort in offices and others commercial environments. Vapor compression refrigeration systems (VCRS) are used mainly for convenience, since this system only requires the largely available electrical power. However, high power consumption can lead to electrical distribution network peaks, according to Wells and Haas (2004) and Opoku *et al.* (2019), mainly because the air-conditioning alone can consume as much as 60% to 80% of building electrical power, in agreement to Kassas (2015). An absorption refrigeration system (ARS) uses far less electrical power, depending only on thermal power to drive the system. Industries can benefit from the residual heat eliminated in some processes to power their cooling systems and increase their viability.

In the literature, some researches were developed to study the thermodynamics involving ARS or VCRS. Narváez-Romo *et al.* (2017) made an extensive review of heat and mass transfer correlations in ARS using ammonia-water or water-lithium bromide working pairs. Braga Martins and Figueiredo (2019) simulated a system with 7.1 kW of cooling capacity adopting global heat transfer rate and experimental data to improve the system COP by up to 31%. In a similar way, Hmida *et al.* (2019) defined a model to analyze the cooling effect of a single effect ARS used in a room, with 8 kW of refrigeration capacity, achieving system coefficient of performance (COP) of 0.72-0.74 when temperatures of generator and evaporator were 120°C and 2°C, respectively. Narváez-Romo and Simões-Moreira (2019) and Narváez-Romo *et al.* (2020) presented an analysis of heat transfer in the absorption process, while Narváez-Romo (2020) investigated experimentally the details of heat transfer rate in the generator and absorber, as well as the heat losses, in ARS with 1.5 kW of cooling capacity.

Those studies were developed applying ammonia-water mixture as working fluid.

Huirem and Sahoo (2020) investigated the system COP and thermodynamic parameters optimizations in a single effect ARS using water-lithium bromide (H_2O-LiBr) with cooling load of 17.5 kW. The first and second laws were employed to model the system. The work of Kadyan *et al.* (2021) presented the simulation of ARS using H_2O-LiBr with 5 kW cooling capacity to study the implementation of an optimizer. Ebrahimnataj Tiji *et al.* (2020) used Engineering Equation Solver (EES) and MATLAB software to simulate and optimize the start-up time and transient conditions of an ARS using ammonia-water or water-lithium bromide working pairs. The usage of an optimized heat exchanger provided improvement over transient aspects of COP and heat transfer rate in generator and condenser, reducing the start-up time.

Chen *et al.* (2019) simulated an ARS integrated with VCRS only using ammonia-water and R-134a as working fluids, respectively. Herrera-Romero and Colorado-Garrido (2020) compared working pairs to drive a compression-absorption refrigeration system. They analyzed the influence of each heat exchanger with cooling load of 50 kW and temperatures in generator, evaporator and condenser of 90°C, -10°C and 40°C, respectively, resulting in COP of 0.36-0.65 for absorption cooling cycle and COP of 6.21-6.62 for vapor compression refrigeration cycle. A method to equal cooling systems driven by thermal (residual heat, for example) or electrical energy was presented by Rocha *et al.* (2012). It is based on primary energy saving index and could be applied on these integrated systems.

Other studies compared different working pairs from those already exposed using thermodynamic simulation, as the work proposed by Khelifa *et al.* (2021), which correlated their results with system COP. Zhang *et al.* (2021) studied the combination of thermally regenerative batteries based on ammonia with an ARS requiring three different fluids: NH_3/$LiNO_3$/LiBr. The thermodynamic model proved ARS could be powered by these batteries.

Also, the integration of an ARS with other systems is common to work with different thermal energy sources or even to increase the viability and benefits of power generation plants and desalinization systems, for example. Souza *et al.* (2020) developed a model using EES to study the integration of an ARS with organic Rankine cycle, while Hernández-Magallanes *et al.* (2021) investigated the overall COP of a system integrating an ARS (as heat pump and cooling system) with a power generation design. The research developed by Tashtoush and Qaseem (2021) explored the variation of characteristics in an ARS integrated with thermoelectric generator to examine possible optimizations.

These researches found in open literature do not focus on comparison between absorption and vapor compression cooling systems directly, using the same operating conditions for both and with the same refrigerant fluid. This proposed investigation can be a great tool to verify which system has more benefits in different situations, such as a lower evaporator temperature. This way, the present work aims to simulate and compare two different types of cooling systems: single stage ammonia-water absorption and vapor compression refrigeration (working with R-134a or R-717) systems. The thermodynamic simulation was carried out by using the Engineering Equation Solver (EES). Heat transfer rates of main devices, coefficients of performance for both systems and specific areas of condenser and evaporator were evaluated.

2. THERMODYNAMIC MODELS

The proposed single effect absorption refrigeration system works with ammonia-water mixture, while the vapor compression refrigeration system (VCRS) uses R-134a or R-717 (anhydrous ammonia) as refrigerant. The thermodynamic models of these systems were developed in EES with thermodynamic properties calculated by the standard library of this software.

The initial conditions applied only for both refrigeration systems are shown in Tab. 1. Two subsystems were defined to work with them: (i) cooling subsystem for condenser; (ii) heat exchanger subsystem for evaporator. The condenser cooling subsystem is presumed to be a heat exchanger type shell and tube, containing liquid mixture with 30% ethylene-glycol and 70% water (EGW). The evaporator heat exchanger subsystem is supposed to be also shell and tube working with the same mixture. For instance, initial conditions for them are expressed in Tab. 2. Both subsystems were used to predict specific areas of condenser and evaporator. The particularities of each refrigeration systems will be described in the upcoming respective sections.

Table 1. Initial conditions for both refrigeration systems.

Variable	Value
Evaporator cooling capacity	15 kW
Fluid temperature at condenser outlet	40°C
Vapor temperature at generator outlet	110°C
Vapor temperature at Evaporator outlet	-20°C to 10°C, with steps of 5°C

Table 2. Initial conditions for subsystems found on both refrigeration systems.

	Subsystem	
Variable	Condenser cooling	Evaporator energy storage unit
Working fluid	30% EGW(1)	30% EGW(1)
Inlet fluid temperature	29°C	15°C hotter than ammonia temperature in evaporator inlet
Outlet fluid temperature	34°C	10°C hotter than ammonia temperature in evaporator outlet

(1) Liquid mixture of 30% ethylene-glycol with 70% water.

2.1 Absorption refrigeration system

The schematic of the single effect absorption refrigeration system (ARS) is presented in Fig. 1. This technology has the main advantage of power the cooling system with thermal energy, requiring low electrical power. In short, the system is composed by absorber, generator, rectifier, condenser and evaporator, but also includes a pump, two expansion valves and two heat exchangers to work properly. This system has a higher pressure in the lines above expansion valves and pump, connecting heat exchanger 2, generator, rectifier and condenser, as can be noted in Fig. 1. The lower pressure reaches the lines attaching absorber, evaporator and heat exchanger 1.

Starting from absorber, refrigerant coming from evaporator is mixed up with weak solution arising from generator and rectifier, resulting in strong solution and producing heat (that must be dissipated) by absorption process. Those three main solutions depend on ammonia content in the ammonia-water mixture. The refrigerant has almost pure ammonia, the weak solution has the lowest ammonia content compared to those three, and the strong solution has higher ammonia content than weak solution, but lower than the refrigerant. These last two solutions are in liquid state. Back to the cycle, strong solution is pumped towards generator, where thermal energy is introduced to vaporize most part of ammonia available in the strong solution, generating vapor with high ammonia content.

Heat must be rejected in the rectifier to increase ammonia purity, generating the refrigerant that is liquefied inside the condenser. After, expansion valve 1 reduces the fluid temperature and pressure by Joule-Thomson effect, changing from about 15 bar to approximately 2 bar, and also decreases its temperature when rejecting heat in the heat exchanger 1. In the evaporator, refrigerant vaporizes as it absorbs the cooling load, and its temperature is increased inside the heat exchanger 1. Then, it flows towards the absorber, where it is mixed up with weak solution, as explained before. In the generator and rectifier, weak solution exits and its temperature is lowered after transferring heat in the heat exchanger 2. Its pressure (and temperature) also decreases when passing through expansion valve 2. After reaching the absorber, the cycle starts again.

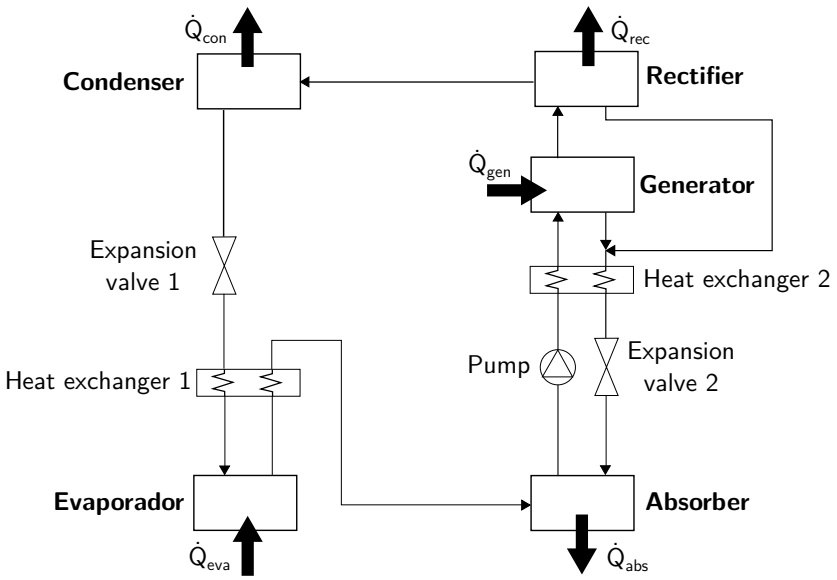

Figure 1. Schematic view of the single effect absorption refrigeration system analyzed.

The thermodynamic model was developed applying energy and mass conservation laws on each device. As extra initial condition, the fluid temperature in the absorber outlet is 23°C. The mass fraction of strong and weak solution has different values but remained constant across all devices, except in the absorber, generator and rectifier where it changes. Expansions valves were determined as isenthalpic, heat exchangers were specified with 80% of thermal effectivity and the pump with 85% of isentropic efficiency. Pressure drops and heat losses in the system were neglected.

Some boundary conditions also assumed are defined in the Tab. 3. Energy balance inside heat exchangers was similar, and both require some assumptions. In the heat exchanger 1, strong solution properties from evaporator and absorber inlets are unknown. First of all, temperatures of these unknown lines were set as the same as strong solution evaporator outlet and expansion valve 1 outlet temperatures, respectively. Then, their guessed thermodynamic properties were calculated based on the pressure of each segment. The lowest multiplication between mass flux and heat capacity for each heat exchange segment was defined to apply the heat transfer effectivity theory. The suitable thermodynamic properties were finally predicted with the effectivity theory and thermodynamic properties of known lines.

Table 3. Boundary conditions in some device inlet or outlet flows for absorption refrigeration system (ARS).

Variable	Boundary condition
Condenser inlet	saturated vapor
Condenser outlet	saturated liquid and pure ammonia
Evaporator outlet	saturated vapor and pure ammonia
Absorber outlet	saturated liquid
Strong solution generator outlet	saturated vapor
Weak solution generator outlet	saturated liquid
Weak solution rectifier outlet	saturated liquid
Weak solution temperature from rectifier outlet	average between inlet and outlet temperatures of strong solution vapors from rectifier

Thermodynamic simulation gives as results the pump power, the heat rate to dissipate in the rectifier, condenser and absorber, and the heat rate necessary to drive the generator. All of them were calculated based on assumptions already described. The coefficient of performance (COP) of this absorption refrigeration system was determined by Eq. (1).

$$COP_{abs} = \frac{\dot{Q}_{eva}}{\dot{Q}_{gen}} \tag{1}$$

where $\dot{Q}_{eva}$ is the refrigeration thermal load (15 kW, as mentioned before) and $\dot{Q}_{gen}$ the heat transfer rate to generator.

The heat exchanger areas of condenser with rectifier and evaporator were calculated based on logarithmic mean temperature difference and a countercurrent flow in a shell and tube heat exchanger subsystem. The initial conditions were described in the Tab. 2. Condensation and rectifier areas were analyzed together because other absorption refrigeration cycles do not have a rectifier. The global heat transfer coefficients used were 2.1 kW/m^2.K for condenser (or rectifier) and 1.9 kW/m^2.K for evaporator, the average values proposed by Brasil. Ministério do Meio Ambiente (2017) using pure ammonia, also known as R-717 refrigerant. The specific area, then, was defined by Eq. (2).

$$A_{esp} = \frac{A_{device}}{\dot{Q}_{eva}} \tag{2}$$

where A_{esp} is the specific area and A_{device} the heat exchanger area from condenser (with rectifier) or evaporator.

2.2 Vapor compression technology

The VCRS simulated is shown in Fig. 2. Note that it has less devices than ARS. Electrical power is given to compressor, which compress the R-134a or R-717 refrigerant, and drives it to condenser, where it lowers its temperature and changes to liquid state. An expansion valve is used to lower the fluid pressure, which enters the evaporator with low pressure and temperature. There, refrigerant vaporizes as absorbs the cooling load and is redirected towards compressor.

The VCRS thermodynamic model was similar to ARS one. It was developed applying energy and mass conservation laws on each device. Initial conditions were defined as expressed in Tab. 1. Pressure drops and heat losses from the system were neglected, and compressor isentropic efficiency was presumed to be 85%. Some boundary conditions were assumed, as defined in Tab. 4.

Thermodynamic simulation gives as results the compressor power and the heat rate required to be dissipated in condenser. All of them were calculated based on assumptions already described. The VCRS COP was determined by Eq. (3).

$$COP_{com} = \frac{\dot{Q}_{eva}}{\dot{W}_{com}} \tag{3}$$

where $\dot{Q}_{eva}$ is the refrigeration thermal load (15 kW, as mentioned before) and $\dot{W}_{com}$ the compressor power required to drive the system.

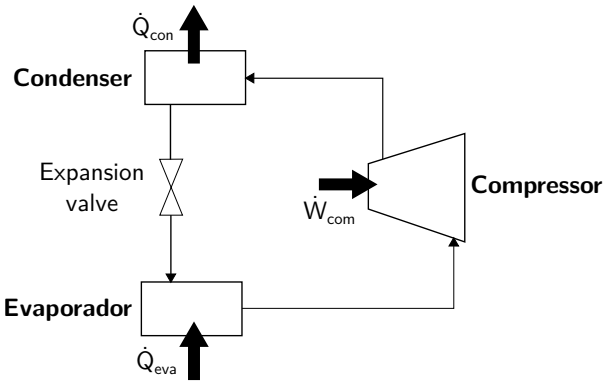

Figure 2. Schematic view of the vapor compression refrigeration system analyzed.

Table 4. Boundary conditions in some device inlet or outlet flows for vapor compression refrigeration system (VCRS).

Variable	Boundary condition
Condenser outlet	saturated liquid
Evaporator outlet	saturated vapor
Evaporator outlet temperature	the same as evaporator inlet
Evaporator outlet pressure	the same as evaporator inlet

Condenser and evaporator heat exchanger areas were calculated based on logarithmic mean temperature difference and a countercurrent flow in a shell and tube heat exchanger subsystem. The initial conditions were described in the Tab. 2. The global heat transfer coefficients used were the average values proposed by Brasil. Ministério do Meio Ambiente (2017). Using R-134a refrigerant those numbers are 1.6 kW/m^2.K for condenser and 0.9 kW/m^2.K for evaporator, while using R-717 these values are 2.1 kW/m^2.K for condenser and 1.9 kW/m^2.K for evaporator. The specific area, then, was defined by Eq. (2).

3. RESULTS AND DISCUSSION

Fig. 3 shows heat transfer rates in the main devices, and also presents the ARS COP. Comparisons were related to the decrease of evaporator temperature. The generator heat rate necessary to drive the ARS increases from 25.0 kW to 41.8 kW as absorber heat dissipated in the environment also increases from 19.2 kW to 36.7 kW. Heat transfer rate of condenser and rectifier remains almost the same, between 14.2-14.4 kW and 6.30-6.38 kW, respectively, while COP decreases from 0.601 to 0.359. The specific areas (area per kW of refrigeration load - kWr) are demonstrated in the Fig. 4. Condenser (with rectifier) and evaporator specific areas remains almost the same, changing between 0.0788-0.0798 m^2/kWr and 0.0423-0.0426 m^2/kWr, respectively.

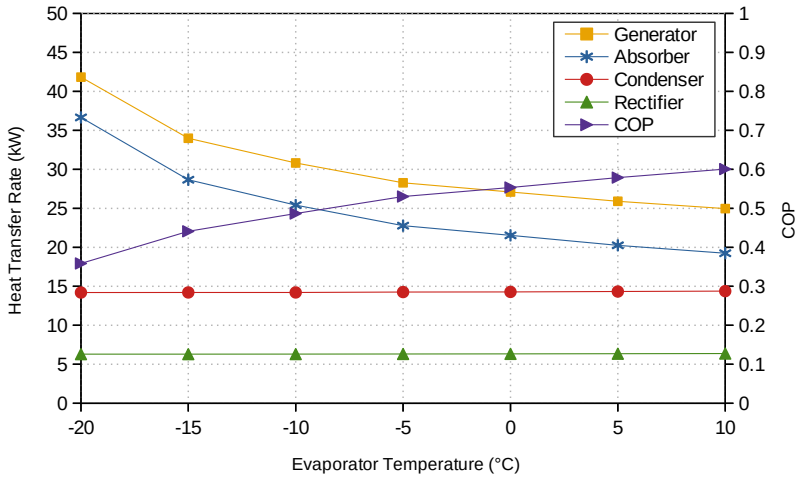

Figure 3. Heat transfer rates from generator, absorber, condenser and rectifier, and coefficient of performance (COP) of absorption refrigeration system (ARS), according to different evaporator temperatures.

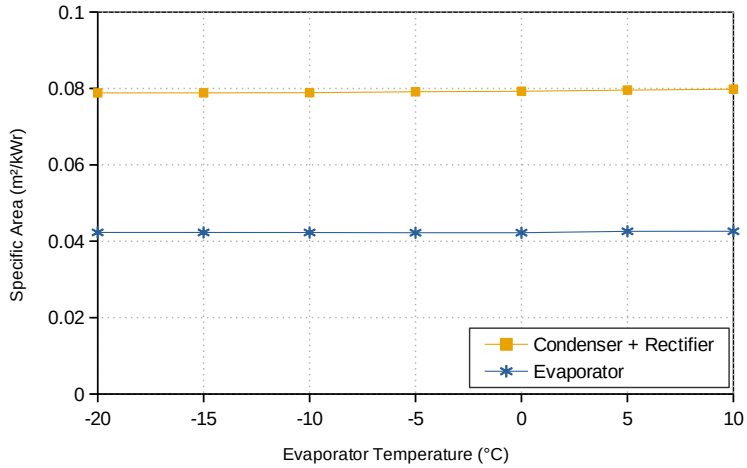

Figure 4. Condenser (with rectifier) and evaporator specific areas of ARS related to evaporator temperature.

Compressor power and condenser heat rate dissipation required for VCRS are presented by Fig. 5. Working with R-134a refrigerant, as evaporator temperature decreases, compressor power increases from 2.22 kW to 5.76 kW and condenser heat dissipation increases from 16.9 kW to 19.9 kW. Using the same comparison parameter, COP decreases from 6.77 to 2.60. Fig. 6 indicates that condenser specific area decreases from 0.0700 to 0.0649 m^2/kWr, while evaporator specific area remains the same value, 0.0901 m^2/kWr.

For the system working with R-717, the values were slightly different. As evaporator temperature decreases, compressor power increases from 2.12 kW to 5.38 kW, condenser heat dissipation increases from 16.8 kW to 19.6 kW and COP decreases from 7.07 to 2.79. Fig. 6 is indicating that condenser specific area decreases from 0.0228 to 0.0152 m^2/kWr, while evaporator specific area remains the same value, 0.0427 m^2/kWr.

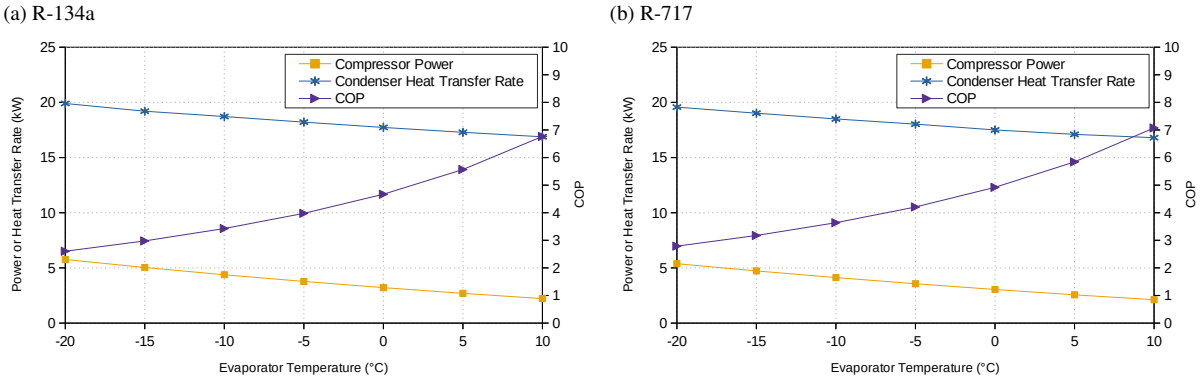

Figure 5. Compressor power, condenser heat transfer rate and coefficient of performance (COP) of vapor compression refrigeration system (VCRS), according to different evaporator temperatures: (a) is the system working with R-134a refrigerant and (b) with R-717 (anhydrous ammonia).

The results for VCRS using R-134a or R-717 has minor changes, and hereafter they will be mentioned together, with standard number-number. When considerable changes were found, they will be treated separated, as an exception. Comparing the two cooling systems, as evaporator temperature reduces from 10°C to -20°C, COP for ARS decreased by 40.3%, while VCRS decreased 60.6-61.5%, which means ARS COP is less susceptible to evaporator temperature, even when comparing the systems working with the same refrigerant. However, VCRS COP tends to be 10 times higher than ARS COP. For both systems, the coefficients of performance calculated using this thermodynamic model were similar to those found by Hmida *et al.* (2019) and Herrera-Romero and Colorado-Garrido (2020).

Generator heat transfer rate for ARS shown an expressive increase of 16.9 kW, or 67.5%, while compressor power for VCRS raised 3.26-3.54 kW, or 154-160%. Although these high percentages for VCRS, the raw values are far lower than ARS. Heat transfer rate of VCRS condenser must reject 2.77-3.02 kW or 17.9% more heat, and for ARS absorber, 17.4 kW or 90.5% increase, and when compared to highest evaporator temperature condition. Those high numbers of heat rates (or low COPs) can be a challenge in the implementation of absorption refrigeration system, meaning this type of cooling technology is appropriated to be employed in locations that have high quantity of heat waste available. This way, many industries can have advantages using waste heat sources instead of electrical power.

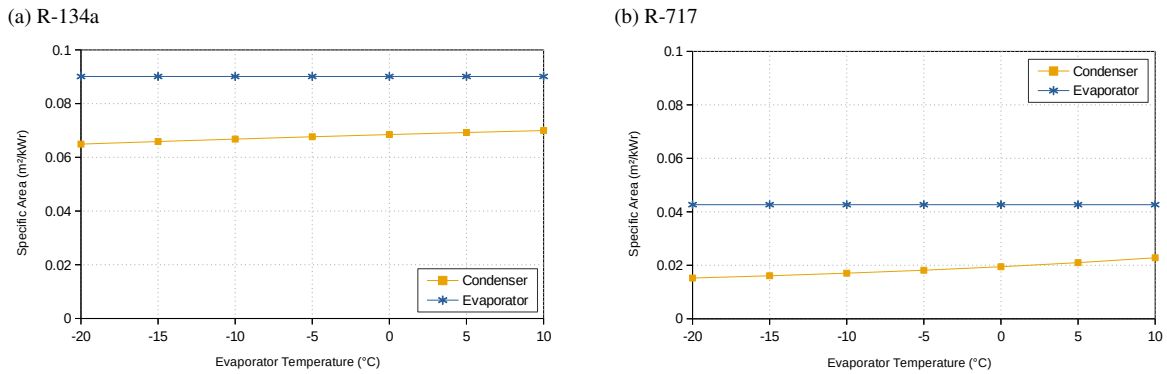

Figure 6. Condenser and evaporator specific areas of VCRS related to evaporator temperature: (a) is the system working with R-134a refrigerant and (b) with R-717.

According to variations of evaporator temperature, ARS and VCRS required specific areas to change up to 7.5%, as shown in Fig. 6. The only exception is condenser specific area of VCRS using R-717, which changed 33.2%. This variation is due to a high increase of ammonia temperature difference (from 36.6 K to 95.5 K) at inlet and outlet of this device, a behavior that is not present on other systems studied even using equal initial conditions.

Analyzing VCRS specific areas when working with R-134a, condenser can be an average of 14.7% smaller and evaporator, around two times smaller compared to ARS. For VCRS using R-717 (ammonia), the same refrigerant used by ARS, specific areas for condenser can be around 76.6% smaller (1/4 of specific size) while evaporator is required to be the same specific size. This last effect is expected, as global heat transfer rate and cooling capacity for evaporator has the same values, heat exchange types are equals and temperature difference at inlet and outlet changes very little. In summary, differences in specific areas are related, not exclusively, to heat transfer coefficients that depend mainly on the refrigerant used and heat exchanger type for condenser and evaporator.

4. CONCLUSIONS

The proposed thermodynamic simulation for both refrigeration systems, a single effect absorption working with ammonia-water and a vapor compression using R-134a or R-717 (anhydrous ammonia), were carried out based on energy and mass conservation laws integrating some initial and boundary conditions. Overall, ARS thermal power value required was greater than VCRS electrical power value. The results of ARS COP were between 0.359-0.601, while VCRS reached between 2.60-6.77 for R-134a and 2.79-7.07 for R-717. Those numbers were similar to other works found in literature and they can, in a future work, be evaluated using the methodology presented by Rocha *et al.* (2012) to equal residual thermal energy with electricity.

As evaporator temperature decreases, absorption refrigeration system (ARS) required up to 16.9 kW, or 67.5%, more heat rate in generator, but must dissipate 17.4 kW or 90.5% more heat rate in absorber. COP decreased by up to 40.3% and heat transfer rates of condenser and rectifier do not had considerable changes. Utilizing the same comparison parameter, the vapor compression refrigeration system (VCRS) needed up to 3.26-3.54 kW, or 154-160%, more compressor power and COP decreased up to 60.6-61.5%. Compared to ARS, condenser specific area required for VCRS is smaller, evaporator can be two times smaller when using R-134a, and need to be equal when using R-717. This effect is highly dependent on the type of refrigerant and heat exchanger.

In summary, ARS has higher increase of generator heat input rate compared to compressor power in the VCRS, as evaporator temperature decreases. Opposite trend is observed when comparing the COP, which means ARS COP changes less than VCRS one when working with the same evaporator temperature variation and refrigerant. Those characteristics justify the usage of ARS in industries or facilities with high amounts of heat waste, where electrical power can be saved, mainly on applications working with lower evaporator temperatures.

5. ACKNOWLEDGEMENTS

This study was financed in part by the Coordenação de Aperfeiçoamento de Pessoal de Nível Superior - Brasil (CAPES) - Finance Code 001. The third author thanks to Fundação de Amparo à Pesquisa do Estado de São Paulo (FAPESP) for the scholarship, n. 2020/08211-4, and the Thematic Project financing, 2016/09509-1. Also, this author thanks the Departamento Administrativo de Ciencia, Tecnología, e Innovación de Colombia – COLCIENCIAS.

6. REFERENCES

Braga Martins, K.R.S. and Figueiredo, J.R., 2019. "Computational simulation and optimization methodology of an ammonia–water GAX absorption cooling system". *Journal of the Brazilian Society of Mechanical Sciences and Engineering*, Vol. 41, No. 11, p. 507.

Brasil. Ministério do Meio Ambiente, 2017. *Ar condicionado: manual sobre sistemas de água gelada : conceitos sobre chillers e sistemas de água gelada / Ministério do Meio Ambiente, Secretaria de Mudança do Clima e Florestas, Departamento de Monitoramento, Apoio e Fomento de Ações em Mudança do Clima.*, Vol. 1 of *3*. MMA.

Chen, W., Li, Z., Sun, Q. and Zhang, B., 2019. "Energy and exergy analysis of proposed compression-absorption refrigeration assisted by a heat-driven turbine at low evaporating temperature". *Energy Conversion and Management*, Vol. 191, pp. 55–70.

Ebrahimnataj Tiji, A., Ramiar, A. and Ebrahimnataj, M., 2020. "Comparison the start-up time of the key parameters of aqua-ammonia and water–lithium bromide absorption chiller (AC) under different heat exchanger configurations". *SN Applied Sciences*, Vol. 2, No. 9, p. 1522.

Hernández-Magallanes, J.A., Tututi-Avila, S., Cerdán-Pasarán, A., Morales, L.I. and Rivera, W., 2021. "Thermodynamic simulation of an absorption heat pump-transformer-power cycle operating with the ammonia-water mixture". *Applied Thermal Engineering*, Vol. 182, p. 116174.

Herrera-Romero, J.V. and Colorado-Garrido, D., 2020. "Comparative Study of a Compression–Absorption Cascade System Operating with NH3-LiNO3, NH3-NaSCN, NH3-H2O, and R134a as Working Fluids". *Processes*, Vol. 8, No. 7, p. 816. Number: 7 Publisher: Multidisciplinary Digital Publishing Institute.

Hmida, A., Chekir, N., Laafer, A., Slimani, M.E.A. and Ben Brahim, A., 2019. "Modeling of cold room driven by an absorption refrigerator in the south of Tunisia: A detailed energy and thermodynamic analysis". *Journal of Cleaner Production*, Vol. 211, pp. 1239–1249.

Huirem, B. and Sahoo, P.K., 2020. "Thermodynamic Modeling and Performance Optimization of a Solar-Assisted Vapor Absorption Refrigeration System (SAVARS)". *International Journal of Air-Conditioning and Refrigeration*, Vol. 28, No. 01, p. 2050006. Publisher: World Scientific Publishing Co.

Kadyan, H., Berwal, A.K. and Mishra, R.S., 2021. "Thermodynamic mathematical modelling and analysis of vapour absorption refrigeration system using a novel ant lion optimiser". *International Journal of Ambient Energy*, Vol. 0, No. 0, pp. 1–14. Taylor & Francis.

Kassas, M., 2015. "Modeling and Simulation of Residential HVAC Systems Energy Consumption". *Procedia Computer Science*, Vol. 52, pp. 754–763.

Khelifa, S., Ramadan, K., Ammar, M.A.H. and Moundji, H.M., 2021. "Performance evaluation of an absorption refrigeration system using R1234yf - organic absorbents working fluids". *Science and Technology for the Built Environment*, Vol. 0, No. 0, pp. 1–18. Taylor & Francis.

Narváez-Romo, B., 2020. *An experimental study of an ammonia-water absorption refrigeration cycle using a novel modified horizontal liquid film absorption system*. Phd thesis, Universidade de São Paulo.

Narváez-Romo, B., Chhay, M., Zavaleta-Aguilar, E.W. and Simões-Moreira, J.R., 2017. "A critical review of heat and mass transfer correlations for LiBr-H2O and NH3-H2O absorption refrigeration machines using falling liquid film technology". *Applied Thermal Engineering*, Vol. 123, pp. 1079–1095.

Narváez-Romo, B., Leite, B.M. and Simões-Moreira, J.R., 2020. "Ammonia-water absorption process on falling films at vertical and inclined plates". *Heat Transfer Research*, Vol. 51, No. 4, pp. 297–318.

Narváez-Romo, B. and Simões-Moreira, J.R., 2019. "Numerical study of heat and mass transfer absorption processes using a horizontal flooded-liquid film in ammonia-water mixtures." In *Proceedings of the 25th IIR International Congress of Refrigeration*. IJR, Montréal , Canada, p. 1269.

Opoku, R., Edwin, I.A. and Agyarko, K.A., 2019. "Energy efficiency and cost saving opportunities in public and commercial buildings in developing countries – The case of air-conditioners in Ghana". *Journal of Cleaner Production*, Vol. 230, pp. 937–944.

Rocha, M., Andreos, R. and Simões-Moreira, J., 2012. "Performance tests of two small trigeneration pilot plants". *Applied Thermal Engineering*, Vol. 41, pp. 84–91. ISSN 13594311. doi:10.1016/j.applthermaleng.2011.12.007. URL `https://linkinghub.elsevier.com/retrieve/pii/S1359431111007046`.

Souza, R.J., Dos Santos, C.A.C., Ochoa, A.A.V., Marques, A.S., Neto, J.L.M. and Michima, P.S.A., 2020. "Proposal and 3E (energy, exergy, and exergoeconomic) assessment of a cogeneration system using an organic Rankine cycle and an Absorption Refrigeration System in the Northeast Brazil: Thermodynamic investigation of a facility case study". *Energy Conversion and Management*, Vol. 217, p. 113002.

Tashtoush, B. and Qaseem, H., 2021. "An integrated absorption cooling technology with thermoelectric generator powered by solar energy". *Journal of Thermal Analysis and Calorimetry*.

Wells, J. and Haas, D., 2004. *Electricity Markets: Consumers Could Benefit from Demand Programs, But Challenges Remain*. DIANE Publishing.

Zhang, S., Luo, J., Xu, Y., Chen, G. and Wang, Q., 2021. "Thermodynamic analysis of a combined cycle of ammonia-based battery and absorption refrigerator". *Energy*, Vol. 220, p. 119728.

7. RESPONSIBILITY NOTICE

The authors are solely responsible for the printed material included in this paper.